

# Solvable model for electrolytic soap films: the two-dimensional two-component plasma

Gabriel Téllez\* and Lina Merchán†

*Departamento de Física, Universidad de Los Andes, A.A. 4976, Bogotá, Colombia*

We study a toy model for electrolytic soap films, the two-dimensional two-component plasma. This model is exactly solvable for a special value of the coulombic coupling constant  $\beta q^2 = 2$ . This allows us to compute the disjoining pressure of a film and to study its stability. We found that the Coulomb interaction plays an important role in this stability. Also the adhesivity that measures the attraction of soap anions to the boundaries is very important. For large adhesivity the film is stable, whereas for small adhesivity a collapse could occur. We also study the density and correlations in the film. The charge density near the boundary shows a double layered profile. We show that the charge correlations verify a certain number of sum rules.

PACS numbers: 5.20.Jj, 68.15.+e, 61.20.Qg, 05.70.Np

Keywords: soap films, Coulomb systems, disjoining pressure, charge density, correlations

## I. INTRODUCTION

When soap molecules interact with water they dissociate into anions and cations. The soap anions have a hydrophilic head and a hydrophobic tail. Therefore, their negative tails prefer to lie on the surface of the film while the positive ions can remain throughout the film. Soap films have a simple configuration and a well defined double layered structure, hence constituting an excellent system to be modeled by a Coulomb gas in a confined geometry. We are interested in the Coulomb interaction between the ions of a two-dimensional soap film and how it contributes to the collapse to a black film.

A soap film, when subject to certain circumstances, may collapse to a thickness smaller than visible light wave length and therefore it is seen black. This phenomenon was observed in the experiments held by O. Belorgey and J. J. Benattar [1] and later by D. Sentenac and J. J. Benattar [2]. In both cases, salt was added to the soap solution. Depending on both the salt concentration and temperature, if the external pressure was increased to a certain point the soap film collapsed to either a Common Black Film (CBF) or to a Newton Black Film (NBF). According to O. Belorgey and J. J. Benattar [1], the CBF equilibrium thickness is due to a balance among attractive van der Waals forces and repulsive forces between the layers. It is believed that short range repulsive forces associated to the local structure of water are responsible for the NBF stability. The sole difference between these two kinds of black films is the thickness of the water layer. The CBF water layer is more than seven times as thick as the NBF water layer. But the external lipid layer has the same width in both black films. In spite of this, the structure and forces involved in black films are not completely understood. We want to know if the

coulombic forces play a role in this phenomenon.

In 1997, the mean field Poisson-Boltzmann theory was applied by Dean and Sentenac [3] to three-dimensional soap films. Within this framework, they studied the disjoining pressure of the soap film for a wide range of salt concentrations and widths of the film. This disjoining pressure is the difference between the external and internal pressures of the film. However, the phenomenon of collapse could not be explained by this mean field approach. Later Dean, Horgan and Sentenac [4] used a functional integral technique to examine a solvable one-dimensional Coulomb system model for a soap film. They found the film charge distribution and discussed the stability criterion for the one-dimensional film. In that model they observed the collapse of the film, so one of their conclusions was that electrostatic forces play an important role in this phenomenon.

In order to see what aspects are particular to the one-dimensional model and what aspects are more general we study here another type of solvable model for a Coulomb system that can be applied to soap films. Working in the framework of classical statistical mechanics, we will model the soap film as a symmetric two-dimensional two-component plasma, i.e, a neutral system of positive and negative particles of opposite charges  $\pm q$  embedded in a neutral background. We are only interested in the role that the Coulomb interaction plays in the collapse of the film so forces like van der Waals and others will not be considered. We will only consider salt-free systems. Also, the internal structure of the particles will not be regarded. This model is exactly solvable for a temperature given by  $q^2/k_B T = 2$ . The attraction of the anions to the interfaces will be accounted for by a short range attractive potential. We will study a film that has an infinite surface and a finite thickness. The two dimensions to be considered lie on the breadth of the film, so this system is invariant in one of the two dimensions. We will study separately the inner and outer regions of the film. For this reason we will use two models. Each one is meant to be used to analyze one of the two regions.

The outline of this paper is as follows. First, in Sec. II

\*Electronic address: gtellez@uniandes.edu.co

†Electronic address: l-mercha@uniandes.edu.co

we will describe the two models we employ. Then, there is brief explanation of the two-component plasma theory and of the general method of solution. In Sec. III, we use the technique presented in Sec. II to find the pressure inside the film. Afterward, in Sec. IV, we will show how to compute the one-particle densities and the truncated two-body densities. Each calculation is followed by its corresponding analysis. Finally, we conclude on the role that electrostatic forces play in the collapse of this two-dimensional soap film.

The main interest of our work is to study a solvable model for a soap film. Given the limitations of this two-dimensional model, we can only compare qualitatively the structure and behavior of this film to a real one.

## II. THE MODEL AND METHOD OF RESOLUTION

In this section, we will present the two models we employed to study a two-dimensional soap film. The two models have a lot in common. Both are two dimensional systems of particles of charge  $\pm q$  confined in a slab of impenetrable walls. This aspect is modeled by an infinite external potential outside the slab. The anions, negatively charged, tend to lie on the external surface of the film. This is accounted for by an attractive short range potential of different form in each model. The cations, on the other hand, can lie anywhere in the film and this is represented by a constant potential. This potential is the same in the two models.

In the first model (model I), the short range potential is modeled by a delta function, while in model II, it is modeled by a step function. The first model will be used to find the pressure and the densities in the inner region of the film whilst the second model will be employed in the computation of the correlations and the densities in the outer layers of the film.

In two dimensions, the Coulomb interaction potential of a charge  $sq$  at a distance  $r$  from another charge  $s'q$  is logarithmic, of the form  $v(r) = -ss'q^2 \ln(r/d)$ , where  $d$  is an irrelevant length scale. The adimensional coulombic coupling constant is  $\Gamma = \beta q^2$ . For a system of point particles the attraction between pairs of opposite sign will make the system unstable at low temperatures. For this reason the partition function is not well defined for  $\Gamma \geq 2$ . While for  $\Gamma < 2$ , the system is stable against collapse.

Let us review the method described by Jancovici and Cornu [5] for the two-component plasma. We start with the grand partition function

$$\Xi = \sum_{N=0}^{\infty} \frac{1}{N!} \lambda_0^N \int d\mathbf{r}_1 \int d\mathbf{r}_2 \dots \int d\mathbf{r}_N \exp(-\beta H), \quad (2.1)$$

where  $N$  is the number of particles and  $\lambda_0$  is the constant fugacity related to the kinetic energy and the

chemical potential. We consider only neutral configurations: the number of positive particles is equal to the number of negative particles. An external potential can be described by a position dependent fugacity  $\lambda(\mathbf{r}_i) = \lambda_0 \exp(-\beta U_{\text{ext}}(\mathbf{r}_i))$ . In order to avoid divergences we start with a discretized model. The position vector  $\mathbf{r} = (x, y)$  will be represented by a complex number  $z = x + iy$ . The particles lie in two interwoven sublattices  $U$  and  $V$ . The positives particles reside in the sublattice  $U$  with coordinates  $u_i$ , while the negatively charged particles reside in the sublattice  $V$  with coordinates  $v_i$ .

For a specific temperature, given by  $q^2/k_B T = 2$ , this model is exactly solvable. For a configuration with  $N$  positive particles and  $N$  negative particles, using a Cauchy identity, it can be shown that

$$\exp\left(-\beta \sum_{i < j} v(r_{ij})\right) = d^{2N} \left| \left[ \det \frac{1}{u_i - v_j} \right]_{i,j=1,\dots,N} \right|^2. \quad (2.2)$$

Using this fact, the grand partition function can be written as

$$\Xi = \det \begin{vmatrix} 1 & 0 & \dots & \frac{d \lambda(u_1)}{u_1 - v_1} & \frac{d \lambda(u_1)}{u_1 - v_2} & \dots \\ 0 & 1 & \dots & \frac{d \lambda(u_2)}{u_2 - v_1} & \frac{d \lambda(u_2)}{u_2 - v_2} & \dots \\ \vdots & \vdots & \ddots & \dots & \dots & \dots \\ \frac{d \lambda(v_1)}{v_1 - u_1} & \frac{d \lambda(v_1)}{v_1 - u_2} & \vdots & 1 & 0 & \dots \\ \frac{d \lambda(v_2)}{v_2 - u_1} & \frac{d \lambda(v_2)}{v_2 - u_2} & \vdots & 0 & 1 & \dots \\ \vdots & \vdots & \vdots & \vdots & \vdots & \ddots \end{vmatrix}. \quad (2.3)$$

If each lattice site is characterized by a complex coordinate  $z$  and by a vector which is  $(1, 0)$  for the positive particles and  $(0, 1)$  for the negative particles then the grand potential can be expressed in the following simplified form

$$\Xi = \det \left[ 1 + \begin{pmatrix} \lambda_+(\mathbf{r}) & 0 \\ 0 & \lambda_-(\mathbf{r}) \end{pmatrix} \begin{pmatrix} 0 & \frac{d}{z - z'} \\ \frac{d}{\bar{z} - \bar{z}'} & 0 \end{pmatrix} \right]. \quad (2.4)$$

with  $\lambda_s$  the fugacity for particles of sign  $s$ .

In the continuum limit where the lattice spacing goes to zero (ignoring divergences for the time being) by using the identity

$$\frac{\partial}{\partial \bar{z}} \frac{1}{z - z'} = \frac{\partial}{\partial \bar{z}} \frac{1}{z - z'} = \pi \delta(\mathbf{r} - \mathbf{r}'), \quad (2.5)$$

it can be shown that

$$\Xi = \det \left[ \begin{pmatrix} 0 & 2\partial_z \\ 2\partial_{\bar{z}} & 0 \end{pmatrix}^{-1} \begin{pmatrix} m_+(\mathbf{r}) & 2\partial_z \\ 2\partial_{\bar{z}} & m_-(\mathbf{r}) \end{pmatrix} \right], \quad (2.6)$$

where  $m_s = \frac{2\pi d}{S} \lambda_s$  are rescaled fugacities ( $S$  is the area of a lattice site). Then defining a new matrix  $K$  as

$$K = \begin{pmatrix} 0 & 2\partial_z \\ 2\partial_{\bar{z}} & 0 \end{pmatrix}^{-1} \begin{pmatrix} m_+(\mathbf{r}) & 0 \\ 0 & m_-(\mathbf{r}) \end{pmatrix}, \quad (2.7)$$

the grand partition function  $\Xi$  can be expressed as

$$\Xi = \det(1 + K). \quad (2.8)$$

The calculation of the pressure,  $p = -\partial\omega/\partial W$ , reduces to finding the eigenvalues of  $K$ . While, on the other hand, the calculation of the one-particle densities and correlations reduces to finding the Green functions  $\mathbf{G}$ , satisfying the following set of equations

$$\begin{pmatrix} m_+(\mathbf{r}_1) & \partial_{x_1} - i\partial_{y_1} \\ \partial_{x_1} + i\partial_{y_1} & m_-(\mathbf{r}_1) \end{pmatrix} \mathbf{G}(\mathbf{r}_1, \mathbf{r}_2) = \delta(\mathbf{r}_1 - \mathbf{r}_2) \mathbf{1}, \quad (2.9)$$

where

$$\mathbf{G} = \begin{pmatrix} G_{++} & G_{+-} \\ G_{-+} & G_{--} \end{pmatrix}, \quad (2.10)$$

and  $\mathbf{1}$  is the unit  $2 \times 2$  matrix, since it can be shown that

$$\rho_{s_1}(\mathbf{r}_1) = m_{s_1} G_{s_1 s_1}(\mathbf{r}_1, \mathbf{r}_1), \quad (2.11a)$$

$$\rho_{s_1 s_2}^{(2)T}(\mathbf{r}_1, \mathbf{r}_2) = -m_{s_1} m_{s_2} G_{s_1 s_2}(\mathbf{r}_1, \mathbf{r}_2) G_{s_1 s_2}(\mathbf{r}_2, \mathbf{r}_1). \quad (2.11b)$$

When an external potential is acting differently on positive and negative particles, it is convenient to define  $m(\mathbf{r})$  and  $V(\mathbf{r})$  as

$$m_s(\mathbf{r}) = m(\mathbf{r}) \exp[-2sV(\mathbf{r})]. \quad (2.12)$$

To symmetrize the problem for the two types of particles, it is useful to define the following modified Green functions

$$g_{s_1 s_2}(\mathbf{r}_1, \mathbf{r}_2) = e^{-s_1 V(\mathbf{r}_1)} G_{s_1 s_2}(\mathbf{r}_1, \mathbf{r}_2) e^{-s_2 V(\mathbf{r}_2)}. \quad (2.13)$$

Using the following operators

$$A = \partial_{x_1} + i\partial_{y_1} + \partial_{x_1} V(\mathbf{r}_1) + i\partial_{y_1} V(\mathbf{r}_1), \quad (2.14a)$$

$$A^\dagger = -\partial_{x_1} + i\partial_{y_1} + \partial_{x_1} V(\mathbf{r}_1) - i\partial_{y_1} V(\mathbf{r}_1), \quad (2.14b)$$

the equations for  $g_{++}$  and  $g_{--}$  decouple into

$$\left\{ m(\mathbf{r}_1) + A^\dagger [m(\mathbf{r}_1)]^{-1} A \right\} g_{++}(\mathbf{r}_1, \mathbf{r}_2) = \delta(\mathbf{r}_1 - \mathbf{r}_2), \quad (2.15a)$$

$$\left\{ m(\mathbf{r}_1) + A [m(\mathbf{r}_1)]^{-1} A^\dagger \right\} g_{--}(\mathbf{r}_1, \mathbf{r}_2) = \delta(\mathbf{r}_1 - \mathbf{r}_2). \quad (2.15b)$$

The other Green functions are given by

$$g_{-+}(\mathbf{r}_1, \mathbf{r}_2) = -[m(\mathbf{r}_1)]^{-1} A g_{++}(\mathbf{r}_1, \mathbf{r}_2) \quad (2.16a)$$

$$g_{+-}(\mathbf{r}_1, \mathbf{r}_2) = [m(\mathbf{r}_1)]^{-1} A^\dagger g_{--}(\mathbf{r}_1, \mathbf{r}_2). \quad (2.16b)$$

We will apply the above method to the models explained next.

The film has a thickness  $W$ . The outer region has a width  $\delta$ , while the inner region has a thickness  $2L$ . The breadth of the film is in the  $x$ -axis and the film is infinite in the  $y$ -axis. The origin is set in the middle of the soap film. Remembering that  $m_s \propto \exp(-\beta U_{\text{ext}}(\mathbf{r}))$ , in model I, the position dependent fugacities are

$$m_+(\mathbf{r}) = m, \quad (2.17a)$$

$$m_-(\mathbf{r}) = m + \alpha(\delta(x - L) + \delta(x + L)). \quad (2.17b)$$

The parameter  $\alpha$  which we will call adhesivity measures the strength of the attractive potential.

Model II differs from the preceding in that the attractive potential acts over a region of length  $\delta$ . For a real soap film, this thickness is approximately the length of the hydrophobic tail. So for this model the position dependent fugacities are

$$m_+(x) = m \quad (2.18a)$$

$$m_-(x) = \begin{cases} m_i & \text{if } x \in [-L - \delta, -L] \cup [L, L + \delta] \\ m & \text{if } x \in [-L, L] \end{cases} \quad (2.18b)$$

with  $m_i = m \exp(-\beta U_{\text{ext}}) > m$  since  $U_{\text{ext}}$  is an attractive constant potential. We can therefore distinguish three regions: the left border  $-L - \delta < x < -L$  (region 1), the bulk of the film  $-L < x < L$  (region 2) and the right border  $L < x < L + \delta$  (region 3).

In this case, the Eqs. (2.15) and (2.16) simplify to

$$\left[ (m(x_1))^2 - \Delta \right] g_{\pm\pm}(x_1, x_2, l) = m(x_1) \delta(x_1 - x_2) \quad (2.19a)$$

$$\frac{1}{m(x_1)} [-\partial_x \mp i\partial_y] g_{\pm\pm}(x_1, x_2, l) = g_{\mp\pm}(x_1, x_2, l) \quad (2.19b)$$

where

$$m(x) = \begin{cases} m_0 = (mm_i)^{1/2} & \text{if } x \text{ in regions 1 or 3,} \\ m & \text{if } x \text{ in region 2.} \end{cases} \quad (2.20)$$

In this model, the potential defined in Eq. (2.12) is the following

$$\exp(V) = \begin{cases} \left(\frac{m_i}{m}\right)^{\frac{1}{4}} & \text{if } x \text{ in regions 1 or 3,} \\ 1 & \text{if } x \text{ in region 2.} \end{cases} \quad (2.21)$$

With this model we will study the case where  $m_i \rightarrow \infty$  and  $\delta \rightarrow 0$  while keeping their product constant. This way model I is a limiting case of model II.

### III. THE PRESSURE

#### A. Formal expression for the grand potential

We shall use here the first model presented in the above section (model I), where the position-dependent fugacity

ties are given by Eqs. (2.17). As explained in the preceding section the grand potential is given by

$$\Xi = \det(1 + K), \quad (3.1)$$

To compute the grand potential we need to find the eigenvalues of  $K$ . The eigenvalue problem for  $K$  with eigenvalues  $\lambda$  and eigenvectors  $(\psi, \chi)$  reads

$$m_-(\mathbf{r})\chi(\mathbf{r}) = 2\lambda\partial_z\psi(\mathbf{r}), \quad (3.2a)$$

$$m_+(\mathbf{r})\psi(\mathbf{r}) = 2\lambda\partial_z\chi(\mathbf{r}). \quad (3.2b)$$

From Eqs. (3.2) and (2.17) we find that  $\chi$  is a continuous function while  $\psi(x, y)$  is discontinuous at  $x = \pm L$  due to the Dirac delta distributions in  $m_-(\mathbf{r})$ . The discontinuity of  $\psi$  is given by Eqs. (3.2a) and (2.17b)

$$\psi(x = \pm L^+, y) - \psi(x = \pm L^-, y) = \frac{\alpha}{\lambda}\chi(x = \pm L, y). \quad (3.3)$$

Inside the film, for  $-L < x < L$ , Eqs. (3.2) can be combined into the Laplacian eigenvalue problem

$$\Delta\chi = \left(\frac{m}{\lambda}\right)^2 \chi. \quad (3.4)$$

Due to the translational invariance in the  $y$ -direction we look for solutions of the form

$$\chi(\mathbf{r}) = (Ae^{-\kappa^*x} + Be^{\kappa^*x})e^{iky}, \quad (3.5)$$

where  $\kappa^* = (k^2 + (m/\lambda)^2)^{1/2}$ . From Eq. (3.2b) we find

$$\psi(\mathbf{r}) = \frac{\lambda}{m}(A(k - \kappa^*)e^{-\kappa^*x} + B(\kappa^* + k)e^{\kappa^*x})e^{iky}. \quad (3.6)$$

Outside the film Eqs. (3.2) reduce to

$$\partial_z\psi = 0 \quad \text{and} \quad \partial_z\chi = 0. \quad (3.7)$$

That is  $\psi$  is analytic and  $\chi$  is antianalytic. Since we are looking for solutions with  $y$  dependence  $e^{iky}$  this gives

$$\psi(\mathbf{r}) = Ce^{kz} = Ce^{kx+iky}, \quad (3.8a)$$

$$\chi(\mathbf{r}) = De^{-k\bar{z}} = De^{-kx+iky}. \quad (3.8b)$$

In order to have vanishing solutions at infinity, from the preceding equations it is necessary that for  $k > 0$

$$\psi(\mathbf{r}) = 0 \quad \text{for } x > L, \quad (3.9a)$$

$$\chi(\mathbf{r}) = 0 \quad \text{for } x \leq -L, \quad (3.9b)$$

and for  $k < 0$

$$\psi(\mathbf{r}) = 0 \quad \text{for } x < -L, \quad (3.9c)$$

$$\chi(\mathbf{r}) = 0 \quad \text{for } x \geq L. \quad (3.9d)$$

Eqs. (3.3) and (3.9) are the boundary conditions that complete the Laplacian eigenvalue problem (3.4). These boundary conditions yield a homogeneous linear system

for the coefficients  $A$  and  $B$ , which in the case  $k > 0$  reads

$$\begin{pmatrix} A & B \end{pmatrix} \begin{pmatrix} (\lambda^2(k - \kappa^*) + \alpha m)e^{-\kappa^*L} & e^{\kappa^*L} \\ (\lambda^2(\kappa^* + k) + \alpha m)e^{\kappa^*L} & e^{-\kappa^*L} \end{pmatrix} = 0. \quad (3.10)$$

In order to have non trivial solutions the determinant of this linear system must vanish. This gives the following equation that must be satisfied by the eigenvalues  $\lambda$

$$(\lambda^2(\kappa^* + k) + \alpha m)e^{2\kappa^*L} + (\lambda^2(\kappa^* - k) - \alpha m)e^{-2\kappa^*L} = 0, \quad (3.11)$$

that can also be written as

$$\cosh(2\kappa^*L) + \left(k + \frac{\alpha m}{\lambda^2}\right) \sinh(2\kappa^*L)/\kappa^* = 0. \quad (3.12)$$

A similar equation is found for the case  $k < 0$  in which one should change  $k$  for  $-k$ . As a consequence of this fact the set of solutions for  $k < 0$  is the same as for  $k > 0$ . From now on we will only consider the case  $k > 0$ .

The grand potential per unit length is then given by

$$\begin{aligned} \beta\omega &= -\frac{1}{2\pi} \int_{-\infty}^{+\infty} \ln \prod_{\lambda_k} (1 + \lambda_k) dk \\ &= -\frac{1}{\pi} \int_0^{+\infty} \ln \prod_{\lambda_k} (1 + \lambda_k) dk, \end{aligned} \quad (3.13)$$

where the product runs over all  $\lambda_k$  solution of Eq. (3.12). This product can actually be performed as explained in refs. [6, 7, 8]. Let us introduce the analytic function

$$\begin{aligned} f_k(z) &= \cosh(2\sqrt{k^2 + m^2z^2}L) \\ &+ (k + \alpha mz^2) \frac{\sinh(2\sqrt{k^2 + m^2z^2}L)}{\sqrt{k^2 + m^2z^2}}. \end{aligned} \quad (3.14)$$

By construction the zeros of  $f_k$  are the inverse of the eigenvalues  $\lambda_k$ . This function  $f_k$  can be factorized as a Weierstrass product running over its zeros. Since  $f_z(0) = \exp(2kL)$ ,  $f'(0) = 0$ ,  $f(z) = f(-z)$  and the zeros of  $f_k$  are  $1/\lambda_k$ , the Weierstrass product representation reduces to

$$f_k(z) = \exp(2kL) \prod_{\lambda_k} (1 - z\lambda_k). \quad (3.15)$$

Then the product appearing in the grand potential (3.13) is simply  $f_k(-1)e^{-2kL}$ . Finally, the grand potential per unit length reads

$$\begin{aligned} \beta\omega &= -\frac{1}{\pi} \int_0^\infty dk \left[ -2kL + \right. \\ &\quad \left. + \ln \left( \cosh(2\kappa L) + \frac{k + \alpha m}{\kappa} \sinh(2\kappa L) \right) \right], \end{aligned} \quad (3.16)$$

where  $\kappa = (k^2 + m^2)^{1/2}$ . The above integral is actually divergent and should be cutoff to a  $k_{\max} \simeq 1/R$  where  $R$

is the diameter of the particles as explained in Ref. [5]. It can be checked that for  $\alpha = 0$ , Eq. (3.16) yields the known grand potential for a two-component plasma in a strip of hard walls [6].

It is interesting to look at the large- $L$  behavior of the grand potential,

$$\omega = -Wp_b + 2\gamma + O(e^{-mW}), \quad (3.17)$$

where  $W = 2L$  is the width of the film, the bulk pressure is given by

$$\begin{aligned} \beta p_b &= \frac{1}{\pi} \int_0^{1/R} (\kappa - k) dk \\ &= \frac{m^2}{2\pi} \left( \ln \frac{2}{mR} + 1 \right), \end{aligned} \quad (3.18)$$

(a known result from Refs. [5, 6], in the limit of vanishing cutoff  $R \rightarrow 0$ ), and the surface grand potential is

$$\beta\gamma = -\frac{1}{2\pi} \int_0^{1/R} \ln \left[ \frac{1}{2} \left( 1 + \frac{k + m\alpha}{\kappa} \right) \right] dk. \quad (3.19)$$

In the limit  $R \rightarrow 0$  the surface grand potential reads

$$\beta\gamma = -\frac{m}{4\pi} \left[ \alpha \ln \frac{2}{mR} + 1 - \pi + \alpha + \frac{1 - \alpha^2}{\alpha} \ln(\alpha + 1) \right]. \quad (3.20)$$

When  $\alpha = 0$  the above expression reduces to the known result [6, 9]

$$\beta\gamma(\alpha = 0) = \frac{m}{2\pi} \left( \frac{\pi}{2} - 1 \right). \quad (3.21)$$

When the cutoff  $R$  vanishes the surface grand potential diverges (except for  $\alpha = 0$ ). This is expected since negative particles are strongly attracted to the boundaries and for point particles this would create divergences in the surface grand potential in addition to the usual divergences in the bulk pressure due to the collapse of particles of opposite sign.

Finally it should be noted in Eq. (3.17) that there are no algebraic corrections in  $1/W$  to the grand potential. The next correction after the surface term is exponentially small. This is the same situation as in a strip with hard walls ( $\alpha = 0$ ) but very different from the situation of ideal conducting boundaries [6] and ideal dielectric boundaries [10]. In those later cases there is indeed an algebraic universal finite-size correction to the grand potential equal to  $\pi/24W$ .

## B. The disjoining pressure

The pressure in the film can be obtained from the grand potential as  $p = -\partial\omega/\partial W$ . The disjoining pressure is defined as the difference between the pressure of the film and the pressure of an infinite system ( $W \rightarrow \infty$ ,

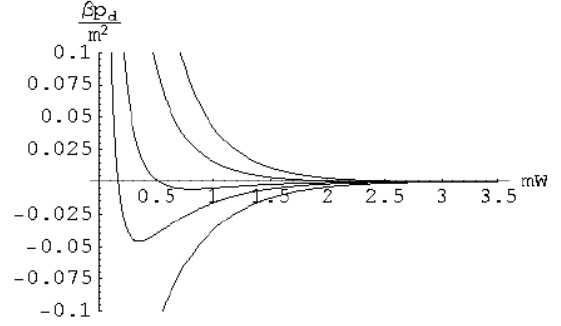


FIG. 1: The disjoining pressure  $p_d$  as a function of the width  $W$  for several values of  $\alpha$ . From top to bottom  $\alpha = 2, 1, 0.5, 0.3, 0$ . Notice that the disjoining pressure becomes positive for small  $W$  except in the case  $\alpha = 0$  where it is always negative.

the bulk pressure):  $p_d = p - p_b$  [4]. Using Eq. (3.16) for the grand potential and Eq. (3.18) for the bulk pressure, we find

$$\beta p_d = \frac{1}{\pi} \int_0^\infty g(k) dk, \quad (3.22a)$$

with

$$g(k) = \frac{2\kappa(-\kappa + k + m\alpha)e^{-2\kappa W}}{\kappa + k + m\alpha + (\kappa - k - m\alpha)e^{-2\kappa W}}. \quad (3.22b)$$

In the limit  $W \rightarrow 0$ , the total pressure is

$$\beta p(W = 0) = \frac{m\alpha}{\pi R}. \quad (3.23)$$

For  $W = 0$  and  $\alpha \neq 0$ , the pressure diverges as  $1/R$  when the cutoff vanishes, stronger than the usual logarithmic divergence. From this fact, it is clear that for  $\alpha \neq 0$  the disjoining pressure will be positive when  $W \rightarrow 0$  (actually  $p_d \rightarrow +\infty$  as  $W \rightarrow 0$ ). The case  $\alpha = 0$  is particular since then the disjoining pressure is of same order as minus the bulk pressure for small- $W$  and then  $p_d \rightarrow -\infty$  when  $W \rightarrow 0$ .

For non-zero width films  $W \neq 0$  the disjoining pressure is finite for vanishing cutoff  $R \rightarrow 0$  (this limit has already been taken in Eq. (3.22)).

Fig. (1) shows several plots of the disjoining pressure as a function of the width  $W$ , for different values of  $\alpha$ . We notice two different behaviors. For  $\alpha = 1$  and  $\alpha = 2$ , the pressure is a monotonous decaying function of the width. This indicates that the film is stable for all widths. For  $\alpha = 0.3$  and  $\alpha = 0.5$ , we notice that the pressure is no longer a monotonous function of the width. There exists a “critical” width  $W_c$  and for  $W > W_c$  the pressure is an increasing function of the width. This indicates that the film is unstable for  $W > W_c$ . Indeed, in that region a small change in the applied pressure to the film will result into a collapse to a width smaller than the critical  $W_c$ . This transition is discontinuous (first order). This

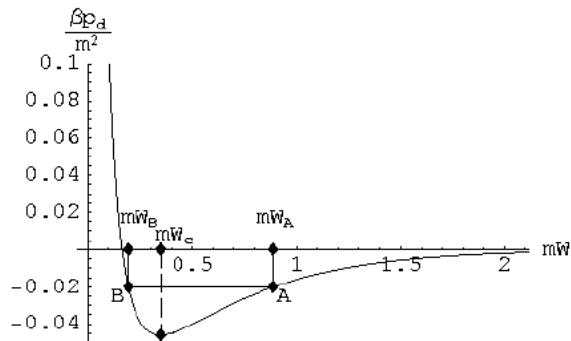


FIG. 2: The disjoining pressure  $p_d$  as a function of the width  $W$  for  $\alpha = 0.3$ . The critical length is  $W_c$ . The phenomenon of collapse is illustrated as follows. Initially the film has a width  $W_A$  corresponding to the point  $A$  in the  $p_d - W$  diagram. A small change in the pressure will force the system to go to point  $B$ : the film has collapsed to a width  $W_B < W_c < W_A$ . This transition is clearly first order (discontinuous).

is illustrated in Fig. (2). In the case  $\alpha = 0$  the disjoining pressure is always negative and increases if  $W$  increases. The film is unstable for all widths when  $\alpha = 0$ .

The critical value of  $\alpha$  distinguishing between these two different behaviors is  $\alpha_c = 1$  as it will be shown below. In order to determine if the pressure is an increasing or decreasing function of  $W$  we study the sign of  $\partial p_d / \partial W$  and in particular the sign of  $\partial g(k) / \partial W$ . We have

$$\frac{\partial g(k)}{\partial W} = \frac{m\kappa^2 [m(1 - \alpha^2) - 2\alpha k] e^{-2\kappa W}}{[\kappa + k + m\alpha + (\kappa - k - m\alpha)e^{-2\kappa W}]^2}. \quad (3.24)$$

Clearly for  $\alpha \geq 1$  the function  $\partial g(k) / \partial W$  is negative for all values of  $k > 0$ , and consequently the disjoining pressure will be a decreasing function of  $W$ .

For  $\alpha < 1$  the function  $\partial g(k) / \partial W$  is positive for values of  $k < k^* = m(1 - \alpha^2) / 2\alpha$  and negative for values of  $k > k^*$ . Since for large values of  $W$ , the function  $\partial g(k) / \partial W$  decays exponentially, the dominant part of the integral in

$$\frac{\partial \beta p_d}{\partial W} = \frac{1}{\pi} \int_0^\infty \frac{\partial g(k)}{\partial W} dk, \quad (3.25)$$

will be given by small values of  $k$ , where  $\partial g(k) / \partial W$  is positive. Then, for large values of  $W$ ,  $\partial p_d / \partial W$  will be positive and  $p_d$  will be an increasing function of  $W$  for large  $W$ .

The exact value of  $W_c$  where  $\partial p_d / \partial W$  changes of sign cannot be determined analytically in a simple manner. However, it can be determined numerically. In Fig. (3) we plot  $W_c$  as a function of the parameter  $\alpha$ .

As a general conclusion of this analysis it can be said that the attractive potential in the boundary of the film, whose strength is characterized by  $\alpha$ , allows the film to stabilize. For  $\alpha > 1$ , films of arbitrary width are stable, whereas for  $\alpha < 1$  only small films are stable, larger films

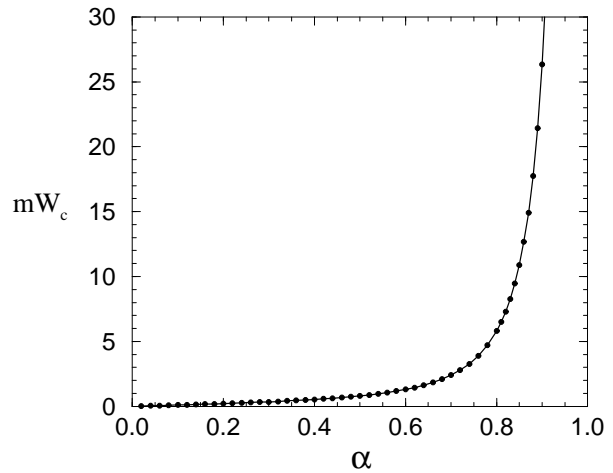


FIG. 3: The critical width  $W_c$  of the films as a function of the adhesivity  $\alpha$ . Films larger than  $W_c$  are unstable.

will collapse, mimicking the collapse to a Common Black Film or to a Newton Black Film in real soap films.

This situation is somehow different to the one exposed in Ref. [4] for a one-dimensional film. Common features of the present study and the one-dimensional case are that for sufficient large values of the adhesivity  $\alpha$  a stable film region exists. For small values of  $\alpha$  ( $\alpha < 1$  in our case) a collapse can occur. But the main difference is that for  $\alpha < 1$  very large two-dimensional films are unstable while very large one-dimensional films are always stable for  $\alpha > 0$ . Another important difference is that in the one-dimensional case multiple collapses are possible whereas in the two-dimensional case we only have one collapse (or no collapse).

#### IV. DENSITY AND CORRELATIONS

The density and correlations can be obtained by computing the Green functions introduced in Sec. II. The present section is divided into two parts. First, we will study the density and correlations inside the film using model I. In the second part, we will compute the density in the boundary of the film and the correlations when one point is on the boundary of the film. For that part we will need to use model II since the Green functions of model I are discontinuous on the boundary as we will see below and therefore do not give any information about the boundary.

## A. Inside the film

### 1. The Green functions

In the present geometry it is natural to work with the Fourier transform  $\hat{G}_{ss'}$  of  $G_{ss'}$  in the  $y$ -direction

$$G_{ss'}(\mathbf{r}_1, \mathbf{r}_2) = \int_{-\infty}^{\infty} \hat{G}_{ss'}(x_1, x_2, k) e^{ik(y_1 - y_2)} \frac{dk}{2\pi}. \quad (4.1)$$

Then Eq. (2.9) translates in Fourier space to

$$\begin{pmatrix} m_+(x_1) & \partial_{x_1} + k \\ \partial_{x_1} - k & m_-(x_1) \end{pmatrix} \hat{\mathbf{G}}(x_1, x_2, k) = \delta(x_1 - x_2) \mathbf{1}. \quad (4.2)$$

Let us detail the calculation of  $G_{--}$  and  $G_{+-}$ , the one for  $G_{++}$  and  $G_{-+}$  follows similar steps. The equations are

$$m\hat{G}_{+-} + (\partial_{x_1} + k)\hat{G}_{--} = 0, \quad (4.3a)$$

$$(\partial_{x_1} - k)\hat{G}_{+-} + m_-(x_1)\hat{G}_{--} = \delta(x_1 - x_2). \quad (4.3b)$$

From Eq. (4.3a) we deduce that  $\hat{G}_{--}$  is continuous. However because of the Dirac delta distributions in the definition of  $m_-$  the function  $\hat{G}_{+-}$  will be discontinuous at  $x_1 = \pm L$ . From Eq. (4.3b) we deduce the discontinuity of  $\hat{G}_{+-}$  at  $x_1 = \pm L$  if  $x_2 \neq x_1$

$$\hat{G}_{+-}(x_1 = \pm L^-) - \hat{G}_{+-}(x_1 = \pm L^+) = \alpha \hat{G}_{--}(x_1 = \pm L), \quad (4.4)$$

If both points  $\mathbf{r}_1$  and  $\mathbf{r}_2$  are inside the film but not on the boundary both fugacities are equal  $m_+ = m_- = m$

and then Eqs. (4.3) can be combined into

$$(\partial_{x_1}^2 - \kappa^2)\hat{G}_{--}(x_1, x_2) = -m\delta(x_1 - x_2), \quad (4.5)$$

with  $\kappa = (k^2 + m^2)^{1/2}$ , while  $\hat{G}_{+-}$  is given by Eq. (4.3a).

If  $\mathbf{r}_1$  is outside the film while  $\mathbf{r}_2$  is fixed inside the film, then  $m_+(x_1) = m_-(x_1) = 0$  and the solution of Eqs. (4.3) is

$$\hat{G}_{--}(x_1, x_2, k) = C e^{-\kappa x_1}, \quad (4.6a)$$

$$\hat{G}_{+-}(x_1, x_2, k) = D e^{\kappa x_1}. \quad (4.6b)$$

In order to have finite solutions at  $x_1 = \pm\infty$  it is necessary that for  $k > 0$

$$\hat{G}_{--}(x_1 \leq -L) = 0 \quad \text{and} \quad \hat{G}_{+-}(x_1 > L) = 0, \quad (4.7a)$$

and for  $k < 0$

$$\hat{G}_{--}(x_1 \geq L) = 0 \quad \text{and} \quad \hat{G}_{+-}(x_1 < -L) = 0. \quad (4.7b)$$

Eqs. (4.4) and (4.7) are the boundary conditions that complement the differential equations (4.3) for the Green functions.

The solution is of the form

$$\hat{G}_{--}(x_1, x_2) = \frac{m}{2\kappa} \left[ e^{-\kappa|x_1 - x_2|} + A e^{-\kappa x_1} + B e^{\kappa x_2} \right], \quad (4.8)$$

where the coefficients  $A$  and  $B$  are determined by the boundary conditions. Finally the Green function  $G_{--}$  is, for  $k > 0$ ,

$$\begin{aligned} \hat{G}_{--}(x_1, x_2, k) = \frac{m}{2\kappa} & \left[ e^{-\kappa|x_1 - x_2|} + \right. \\ & + \frac{-(k + \kappa + \alpha m)e^{-\kappa(x_1 + x_2)} + (\kappa - k - \alpha m)e^{\kappa(x_1 + x_2)}}{(\kappa - k - \alpha m)e^{-\kappa W} + (k + \kappa + \alpha m)e^{\kappa W}} + \\ & \left. + \frac{2(-\kappa + k + \alpha m)e^{-\kappa W} \cosh \kappa(x_1 - x_2)}{(\kappa - k - \alpha m)e^{-\kappa W} + (k + \kappa + \alpha m)e^{\kappa W}} \right], \quad (4.9a) \end{aligned}$$

and for  $k < 0$ ,

$$\begin{aligned} \hat{G}_{--}(x_1, x_2, k) = \frac{m}{2\kappa} & \left[ e^{-\kappa|x_1 - x_2|} + \right. \\ & + \frac{(\kappa + k - \alpha m)e^{-\kappa(x_1 + x_2)} + (-\kappa + k - \alpha m)e^{\kappa(x_1 + x_2)}}{(\kappa + k - \alpha m)e^{-\kappa W} + (\kappa - k + \alpha m)e^{\kappa W}} + \\ & \left. + \frac{2(-\kappa - k + \alpha m)e^{-\kappa W} \cosh \kappa(x_1 - x_2)}{(\kappa + k - \alpha m)e^{-\kappa W} + (\kappa - k + \alpha m)e^{\kappa W}} \right], \quad (4.9b) \end{aligned}$$

and  $\hat{G}_{+-}$  can be obtained from Eq. (4.3a). Similar calculations lead to  $\hat{G}_{++}$  for  $k > 0$ ,

$$\begin{aligned} \hat{G}_{++}(x_1, x_2, k) = & \frac{m}{2\kappa} \left[ e^{-\kappa|x_1-x_2|} + \right. \\ & + \frac{-(\kappa+k) \left(1 - \alpha \frac{\kappa+k}{m}\right) e^{\kappa(x_1+x_2)} + (\kappa-k) \left(1 + \alpha \frac{\kappa-k}{m}\right) e^{-\kappa(x_1+x_2)}}{(\kappa-k-\alpha m)e^{-\kappa W} + (\kappa+k+\alpha m)e^{\kappa W}} + \\ & \left. + \frac{2(k-\kappa+\alpha m)e^{-\kappa W} \cosh \kappa(x_1-x_2)}{(\kappa-k-\alpha m)e^{-\kappa W} + (\kappa+k+\alpha m)e^{\kappa W}} \right], \quad (4.10a) \end{aligned}$$

while for  $k < 0$ ,

$$\begin{aligned} \hat{G}_{++}(x_1, x_2, k) = & \frac{m}{2\kappa} \left[ e^{-\kappa|x_1-x_2|} + \right. \\ & + \frac{(\kappa+k) \left(1 + \alpha \frac{\kappa+k}{m}\right) e^{\kappa(x_1+x_2)} - (\kappa-k) \left(1 - \alpha \frac{\kappa-k}{m}\right) e^{-\kappa(x_1+x_2)}}{(\kappa+k-\alpha m)e^{-\kappa W} + (\kappa-k+\alpha m)e^{\kappa W}} + \\ & \left. + \frac{2(-k-\kappa+\alpha m)e^{-\kappa W} \cosh \kappa(x_1-x_2)}{(\kappa+k-\alpha m)e^{-\kappa W} + (\kappa-k+\alpha m)e^{\kappa W}} \right]. \quad (4.10b) \end{aligned}$$

The Green function  $\hat{G}_{-+}$  is obtained from

$$\hat{G}_{-+}(x_1, x_2) = -\frac{1}{m}(\partial_{x_1} - k)\hat{G}_{++}(x_1, x_2). \quad (4.11)$$

We omit the details of the calculation for  $\hat{G}_{++}$ . Let us only note that in this case,  $\hat{G}_{+-}$  is continuous while  $\hat{G}_{++}$  is discontinuous at  $x_1 = \pm L$  with

$$\hat{G}_{++}(x_1 = \pm L^-) - \hat{G}_{++}(x_1 = \pm L^+) = \alpha \hat{G}_{+-}(x_1 = \pm L). \quad (4.12)$$

The Green functions  $\mathbf{G}(\mathbf{r}_1, \mathbf{r}_2)$  in position space are given by the Fourier transform formula (4.1). The term  $m \exp(-\kappa|x_1-x_2|)/(2\kappa)$  that appears in all  $\hat{G}_{ss}$  give the bulk contribution to  $G_{ss}$  [5]

$$G_{\text{bulk}} = \frac{m}{2\pi} K_0(m|\mathbf{r}_1 - \mathbf{r}_2|), \quad (4.13)$$

where  $K_0$  is the modified Bessel function of the second kind of order 0.

For  $\alpha = 0$  the expressions for the Green functions reduce to known results [11].

## 2. The density

The density of species of charge  $s$  is given by

$$\rho_s(\mathbf{r}) = m_s(\mathbf{r})G_{ss}(\mathbf{r}, \mathbf{r}). \quad (4.14)$$

Using Eqs. (4.9) and (4.10) for the Green functions we obtain the densities

$$\rho_-(x) = \rho_b + \frac{m^2}{\pi} \int_0^\infty \frac{(k-\kappa+\alpha m)e^{-\kappa W} - (k+\alpha m) \cosh(2\kappa x)}{(\kappa-k-\alpha m)e^{-\kappa W} + (\kappa+k+\alpha m)e^{\kappa W}} \frac{dk}{\kappa} \quad (4.15a)$$

$$\rho_+(x) = \rho_b + \frac{m^2}{\pi} \int_0^\infty \frac{(k-\kappa+\alpha m)e^{-\kappa W} - \left(k-\alpha m - \frac{2\alpha k^2}{m}\right) \cosh(2\kappa x)}{(\kappa-k-\alpha m)e^{-\kappa W} + (\kappa+k+\alpha m)e^{\kappa W}} \frac{dk}{\kappa} \quad (4.15b)$$

where  $\rho_b$  is the bulk density (actually divergent when the cutoff  $R \rightarrow 0$ ). The charge density  $\rho = \rho_+ - \rho_-$

(measured in units of  $q$ ) is then

$$\rho(x) = \frac{2m\alpha}{\pi} \int_0^\infty \frac{\kappa e^{-\kappa W} \cosh(2\kappa x) dk}{\kappa+k+\alpha m + (\kappa-k-\alpha m)e^{-2\kappa W}}. \quad (4.16)$$



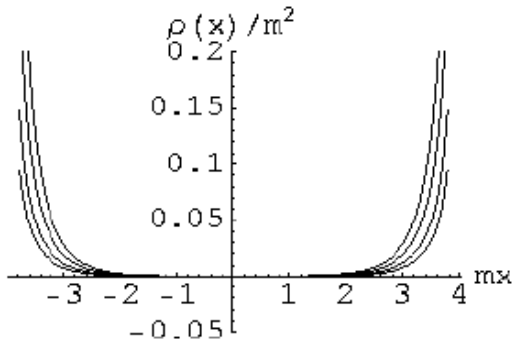


FIG. 4: The charge density as a function of the position  $x$  for several values of  $\alpha$ . The width of the film is  $W = 8/m$ . From top to bottom  $\alpha = 2, 1, 0.5, 0.3$ .

Fig. (4) shows several plots of the charge density as a function of the position  $x$ . This figure can be understood as follows. Because of the strong attractive potential on the boundary an important part of the negative particles (the soap molecules) are stuck in the borders of the film at  $x = \pm L$  creating a layer of negative surface charge density (actually it is really a linear charge density since our system is two-dimensional, in a three-dimensional case it would be a real surface charge density). In the framework of model I, this negative surface charge density cannot be seen in Fig. (4) nor in the analytic expressions found for the densities, but it will be studied in detail in the second part of this section (section IV B) when we will work model II.

The system on the interior of the film is then non-neutral with an excess positive charge. This excess positive charge screens the negative surface charge density at the borders as it can be seen on Fig. (4). The density near the boundary is positive and becomes very large when the boundary is approached. Away from the borders, near the middle of the film, the system is almost neutral. Also in Fig. (4) and from the analytic expression (4.16) for the density it can be checked that the screening length is of order  $m^{-1}$ , a well-known result [5]. It should be noted that for  $\alpha = 0.3$  and  $\alpha = 0.5$  the system should collapse according to the analysis of the preceding section (Sec. III). However there is no hint on the charge density profiles indicating the collapse. This was also the case on the one-dimensional model [4].

The surface charge on one border  $-\sigma$  can be computed by using the screening sum rule

$$\sigma = \int_0^L \rho(x) dx, \quad (4.17)$$

giving

$$\sigma = \frac{\alpha m}{2\pi} \int_0^\infty \frac{(1 - e^{-2\kappa W}) dk}{\kappa + k + \alpha m + (\kappa - k - \alpha m)e^{-2\kappa W}}. \quad (4.18)$$

Actually the above expression is divergent and should be cutoff to a  $k_{\max} \simeq 1/R$  as it has been done for the pressure. In section IV B a more direct calculation of  $\sigma$  will be done and the validity of the screening sum rule will be proven.

The surface charge density  $\sigma$  is an increasing function of  $W$ . Actually for large films it converges exponentially fast to the value

$$\begin{aligned} \sigma_b &= \frac{\alpha m}{2\pi} \int_0^{1/R} \frac{1}{\kappa + k + \alpha m} dk \\ &= \frac{m}{4\pi} \left[ \alpha \ln \frac{2}{mR} - \frac{\alpha^2 + 1}{\alpha} \ln(\alpha + 1) + 1 \right]. \end{aligned} \quad (4.19)$$

The vanishing terms when  $R \rightarrow 0$  have been omitted in the second equality. The dominant term of  $\sigma_b$ , when the cutoff vanishes, is proportional to  $\alpha$ . It is clear that  $\alpha$  controls how much the boundaries get charged.

For very large films  $W \rightarrow \infty$ , it is interesting to study the relationship between the surface charge density  $\sigma_b$  and the surface tension. Actually the surface grand potential  $\gamma$  computed in Sec. III is really the surface tension of the system since we are dealing with polarizable interfaces [5, 12]. This is clear in model II (model I being a special limit of model II) where the particles are free to go from region  $-L < x < L$  to the boundary regions  $-L - \delta < x < -L$  and  $L < x < L + \delta$ . In that model the control parameter for charging the boundaries is the attractive potential  $U_{\text{ext}}$ , or equivalently the fugacity  $m_i$ . For model I the control parameter is the adhesivity  $\alpha$ . From the formal expressions of  $\gamma$  and  $\sigma_b$  given by Eqs. (3.19) and (4.19) it can be verified that

$$\sigma_b = -\beta \alpha \frac{\partial \gamma}{\partial \alpha}, \quad (4.20)$$

which can be regarded as a particular form of Lippmann equation for this model [5].

### 3. The correlations

The truncated two-body correlation function for a particle of sign  $s$  at  $\mathbf{r}_1$  and a particle of sign  $s'$  at  $\mathbf{r}_2$  is given in terms of the Green functions by

$$\rho_{ss'}^{(2)T}(\mathbf{r}_1, \mathbf{r}_2) = -m_s(\mathbf{r}_1)m_{s'}(\mathbf{r}_2)G_{ss'}(\mathbf{r}_1, \mathbf{r}_2)G_{s's}(\mathbf{r}_2, \mathbf{r}_1). \quad (4.21)$$

With the expressions for the Green functions given by Eqs. (4.9) and (4.10) the correlation functions can be obtained.

Due to the screening properties the structure near a boundary will not be modified considerably by the presence of the other boundary. For this reason it is interesting to study in further detail the case of large films  $W \rightarrow \infty$ . The corrections for finite films are exponentially small in  $mW$ .

For  $W \rightarrow \infty$ , taking the origin at the boundary ( $x$  is now changed to  $x + L$ ), the Fourier transforms of the Green functions simplify, for  $k > 0$ , to

$$\hat{G}_{--}(x_1, x_2) = \hat{G}_{\text{bulk}} - \frac{m}{2\kappa} e^{-\kappa(x_1+x_2)}, \quad (4.22a)$$

$$\begin{aligned} \hat{G}_{++}(x_1, x_2) &= \hat{G}_{\text{bulk}} + \\ &+ \frac{m}{2\kappa} \frac{(\kappa - k) \left[1 + \frac{\alpha}{m}(\kappa - k)\right]}{\kappa + k + \alpha m} e^{-\kappa(x_1+x_2)}, \end{aligned} \quad (4.22b)$$

and for  $k < 0$

$$\begin{aligned} \hat{G}_{--}(x_1, x_2) &= \hat{G}_{\text{bulk}} + \\ &+ \frac{m}{2\kappa} \frac{\kappa + k - \alpha m}{\kappa - k + \alpha m} e^{-\kappa(x_1+x_2)}, \end{aligned} \quad (4.22c)$$

$$\begin{aligned} \hat{G}_{++}(x_1, x_2) &= \hat{G}_{\text{bulk}} + \\ &+ \frac{m}{2\kappa} \frac{(k - \kappa) \left[1 - \frac{\alpha}{m}(\kappa - k)\right]}{\kappa - k + \alpha m} e^{-\kappa(x_1+x_2)}. \end{aligned} \quad (4.22d)$$

As a very curious fact it should be noted that the preceding expressions for  $\hat{G}_{--}$  are formally identical with the ones of Ref. [5] for a two-component plasma near a charged hard wall if one chooses in the later case the external surface charge density of the wall equal to  $-\alpha m/(2\pi)$ . This does not mean that in our case the charge density (which is actually not external to the system, but internal and due to the reorganization of charges in the film) is  $-\alpha m/(2\pi)$ . In the preceding subsection we have computed the surface charge density  $-\sigma$  and we know that it is not equal to  $-\alpha m/(2\pi)$ . Furthermore for the Green functions  $\hat{G}_{++}$  this comparison does not hold, the expression for  $\hat{G}_{++}$  given by Eqs. (4.22) and those from Ref. [5] are very different.

It is clear from Eqs. (4.22) that the correlation functions will decay exponentially fast in the  $x$ -direction (through the width of the film). However it is well known that in the  $y$ -direction, parallel to the boundary, the correlation functions usually decay algebraically [13, 14, 15]. For two-dimensional Coulomb systems, near a hard or dielectric (non-conducting) wall, they should decay as  $y^{-2}$ . For a hard wall ( $\alpha = 0$ ) the total charge correlation function  $S(\mathbf{r}_1, \mathbf{r}_2) = \rho_{++}^{(2)T}(\mathbf{r}_1, \mathbf{r}_2) + \rho_{--}^{(2)T}(\mathbf{r}_1, \mathbf{r}_2) - \rho_{+-}^{(2)T}(\mathbf{r}_1, \mathbf{r}_2) - \rho_{-+}^{(2)T}(\mathbf{r}_1, \mathbf{r}_2)$  should behave, for  $y = y_1 = y_2 \rightarrow \infty$ , as [13, 14, 15]

$$S(\mathbf{r}_1, \mathbf{r}_2) \simeq \frac{f(x_1, x_2)}{|y|^2}, \quad (4.23)$$

and the function  $f(x_1, x_2)$  should obey the sum rule

$$\int_0^\infty dx_2 \int_0^\infty dx_1 f(x_1, x_2) = -\frac{1}{2\pi^2\beta}. \quad (4.24)$$

The preceding asymptotic behavior is very general for a Coulomb system near a plane hard wall.

Returning to our case, the Fourier transform of the Green functions have a discontinuity at  $k = 0$  which will translate in position space into a decay as  $1/y$  for

large  $y$ , then the correlation functions will indeed have a decay as  $1/y^2$ . More precisely, the large- $y$  behavior of the charge correlation function is found to be  $S(\mathbf{r}_1, \mathbf{r}_2) \simeq f(x_1, x_2)/y^2$  with the function  $f(x_1, x_2)$  given by

$$f(x_1, x_2) = -\frac{m^2 e^{-2m(x_1+x_2)}}{(\alpha + 1)^2 \pi^2}. \quad (4.25)$$

This function obeys the sum rule

$$\int_0^\infty dx_2 \int_0^\infty dx_1 f(x_1, x_2) = -\frac{1}{2\pi^2\beta(\alpha + 1)^2}. \quad (4.26)$$

According to Ref. [13, 14, 15] for a Coulomb system near a plane hard wall with an external charge density on the wall the sum rule (4.24) is not modified. In our case, where the boundary is charged by a fraction of the particles of the system, the sum rule is modified. However in the sum rule (4.26) we only accounted for the correlations of particles in the fluid. As we will see in Sec. IV B there are also correlations for particles that are absorbed in the boundary and when these are taken into account the sum rule (4.24) is verified.

It is also interesting to comment on the case  $\alpha \rightarrow \infty$ . It can be checked that in that limit Eqs. (4.22) reduce to

$$\hat{G}_{--}(x_1, x_2) = \hat{G}_{\text{bulk}} - \frac{m}{2\kappa} e^{-\kappa(x_1+x_2)}, \quad (4.27a)$$

$$\begin{aligned} \hat{G}_{++}(x_1, x_2) &= \hat{G}_{\text{bulk}} + \\ &+ \frac{(\kappa - k)^2}{2m\kappa} e^{-\kappa(x_1+x_2)}, \end{aligned} \quad (4.27b)$$

for all values of  $k$ . Computing the inverse Fourier transforms gives

$$G_{--}(\mathbf{r}_1, \mathbf{r}_2) = \frac{m}{2\pi} [K_0(mr_{12}) - K_0(mr_{12}^*)] \quad (4.27c)$$

$$\begin{aligned} G_{++}(\mathbf{r}_1, \mathbf{r}_2) &= \frac{m}{2\pi} K_0(r_{12}) + \\ &+ \frac{m}{2\pi} e^{-i\phi_{12}^*} K_2(mr_{12}^*), \end{aligned} \quad (4.27d)$$

where  $r_{12} = |\mathbf{r}_1 - \mathbf{r}_2|$  and  $r_{12}^* = |\mathbf{r}_1 - \mathbf{r}_2^*|$  with  $\mathbf{r}_2^* = (-x_2, y_2)$  being the image of  $\mathbf{r}_2$ . The angle  $\phi_{12}^*$  is the angle of the vector  $\mathbf{r}_1 - \mathbf{r}_2^*$  with respect to the  $x$ -axis.

It is clear that, when  $\alpha \rightarrow \infty$ , the Green functions have no longer an algebraic decay along the  $y$ -direction. The decay is now exponential in all directions and of the form  $\exp(-mr_{12})$  and  $\exp(-mr_{12}^*)$ .

## B. On the boundary of the film

We are now interested in the structure of the film at the boundary. Model I cannot give directly any information on the density or the correlations at the boundary since some of the Green functions are discontinuous there. We

shall use instead model II where the fugacities are given by

$$m_-(x) = \begin{cases} m_i & \text{if } x \in [-L - \delta, -L] \cup [L, L + \delta], \\ m & \text{if } x \in [-L, L], \end{cases} \quad (4.28)$$

and  $m_+(x) = m$  everywhere. Recall that we distinguish between three different regions: the left border  $-L - \delta < x < -L$  (region 1), the bulk of the film  $-L < x < L$  (region 2) and the right border  $L < x < L + \delta$  (region 3).

### 1. The Green functions

It is useful to work with the modified Green functions as explained in Sec. II. As before we will concentrate on the computation of  $g_{--}$ , the one for  $g_{++}$  follows the same lines. We fix the source point  $\mathbf{r}_2$  in region 1. Then, the Green function obeys Helmholtz equation in the different regions

$$(\Delta_{\mathbf{r}_1} - m(x_1)^2)g_{--}(\mathbf{r}_1, \mathbf{r}_2) = -m(x_1)\delta(\mathbf{r}_1 - \mathbf{r}_2), \quad (4.29)$$

and

$$g_{+-}(\mathbf{r}_1, \mathbf{r}_2) = \frac{1}{m(x_1)}(-\partial_{x_1} + i\partial_{y_1})g_{--}(\mathbf{r}_1, \mathbf{r}_2), \quad (4.30)$$

with the position dependent fugacity

$$m(x) = \begin{cases} m_0 = (mm_i)^{1/2} & \text{if } x \text{ in regions 1 or 3,} \\ m & \text{if } x \text{ in region 2.} \end{cases} \quad (4.31)$$

Working with the Fourier transforms  $\hat{g}_{ss'}$  of  $g_{ss'}$  we have, if  $\mathbf{r}_1$  is in region 1,

$$\hat{g}_{--}(x_1, x_2) = \frac{m_0}{\kappa_0} e^{-\kappa_0|x_1-x_2|} + A_1 e^{-\kappa_0 x_1} + B_1 e^{\kappa_0 x_1}, \quad (4.32a)$$

if  $\mathbf{r}_1$  is in region 2,

$$\hat{g}_{--}(x_1, x_2) = A_2 e^{-\kappa x_1} + B_2 e^{\kappa x_1}, \quad (4.32b)$$

and if  $\mathbf{r}_1$  is in region 3,

$$\hat{g}_{--}(x_1, x_2) = A_3 e^{-\kappa_0 x_1} + B_3 e^{\kappa_0 x_1}, \quad (4.32c)$$

with  $\kappa_0 = (m_0^2 + k^2)^{1/2}$ . The coefficients  $A_i$  and  $B_i$  are determined by the following boundary conditions:  $\hat{G}_{ss'}$  should be continuous at  $x_1 = \pm L$  and at  $x_1 = \pm(L + \delta)$ . Furthermore, for  $k > 0$ ,  $\hat{G}_{--} = 0$  if  $x_1 \leq -L - \delta$  and  $\hat{G}_{+-} = 0$  if  $x_1 \geq L + \delta$ . And for  $k < 0$ ,  $\hat{G}_{--} = 0$  if  $x_1 \geq L + \delta$  and  $\hat{G}_{+-} = 0$  if  $x_1 \leq -L - \delta$ . These boundary conditions yield a linear system of six equations for the coefficients  $A_i$  and  $B_i$  for each case  $k > 0$  and

$k < 0$ . This system can be solved by standard matrix manipulation programs like MATHEMATICA. Since the solution is actually not very illuminating and too long to reproduce here we will only consider from now on the limit  $m_i \rightarrow \infty$ ,  $\delta \rightarrow 0$  while  $m_i \delta = \alpha$  is kept constant. This limit is taken after the linear system has been solved. In this limit model II reduces to model I.

In the limiting procedure it is very important to observe how the Green functions scale with the fugacity  $m_i$ . We find that  $g_{--}$  is proportional to  $m_i^{1/2}$  when  $\mathbf{r}_1$  is in region 1. Then the density will be proportional to  $m_i$  and diverges in the limit  $m_i \rightarrow \infty$ . However the “surface” charge density  $\sigma_- = \delta\rho_-$  will have a finite value. Similar scaling behaviors appear in the other regions, giving finite surface charge density-surface charge density  $\langle \sigma_-(\mathbf{r}_1)\sigma_-(\mathbf{r}_2) \rangle$  correlations for both points in boundary region 1, and finite charge density-surface charge density  $\langle \rho_s(\mathbf{r}_1)\sigma_-(\mathbf{r}_2) \rangle$  for  $\mathbf{r}_1$  in region 2 and  $\mathbf{r}_2$  in region 1, as it should be.

On the other hand the function  $\hat{g}_{++}$  for instance is of order  $1/m_i^{1/2}$  when  $\mathbf{r}_1$  and  $\mathbf{r}_2$  are in region 1. This will give a finite charge density  $\rho_+$  in the boundary which is negligible when compared to the surface charge density  $\sigma_-$ . The same holds for correlations when  $\mathbf{r}_1$  is in region 2 and  $\mathbf{r}_2$  in region 1, we find finite charge density-charge density correlations  $\langle \rho_s(\mathbf{r}_1)\rho_+(\mathbf{r}_2) \rangle$  which are negligible when compared to the charge density-surface charge density correlation function  $\langle \rho_s(\mathbf{r}_1)\sigma_-(\mathbf{r}_2) \rangle$ .

This is not surprising. We know from the preceding section that the strong attractive potential has created a negative surface charge density at the boundaries.

The results for the relevant Green functions are, for  $\mathbf{r}_1$  in region 1 and  $k < 0$  (with  $W = 2L$ )

$$\hat{g}_{--} = \frac{m_0(1 - e^{-2\kappa W})}{\kappa - k + \alpha m + (\kappa + k - \alpha m)e^{-2\kappa W}}, \quad (4.33)$$

while for  $k > 0$ ,  $\hat{g}_{--} = O(m_0^{-1})$ . All other Green functions in this region are of order  $O(m_0^{-1})$ .

For  $\mathbf{r}_1$  in region 2 we find, for  $k < 0$ ,

$$\hat{g}_{--}(x_1) = \frac{2(m_0 m)^{1/2} e^{-\kappa W} \sinh \kappa(L - x_1)}{\kappa - k - \alpha m + (\kappa + k - \alpha m)e^{-2\kappa W}}, \quad (4.34a)$$

and

$$\hat{g}_{+-}(x_1) = \left[ \frac{m_0}{m} \right]^{1/2} \times \frac{e^{-\kappa(L+x_1)} [\kappa - k + (\kappa + k)e^{-2\kappa(L-x_1)}]}{\kappa - k + \alpha m + (\kappa + k - \alpha m)e^{-2\kappa W}}, \quad (4.34b)$$

while for  $k > 0$  the Green functions  $\hat{g}_{--}$  and  $\hat{g}_{+-}$  are of order  $O(m_0^{-1/2})$ . Also the other Green functions  $\hat{g}_{++}$  and  $\hat{g}_{-+}$  are of order  $O(m_0^{-1/2})$ .

When  $\mathbf{r}_1$  is in the other boundary (region 3) we found that all Green functions are of order  $O(m_0^{-1})$ .

### 2. The density

We now compute the density on the boundary. Using Eq. (4.33) for the Green function  $g_{--}$  and the formula

$$\rho_s(\mathbf{r}) = m_0 g_{ss}(\mathbf{r}, \mathbf{r}), \quad (4.35)$$

we find a charge density  $\rho_-$  proportional to  $m_i$ . Then the surface charge density  $\sigma_- = \delta\rho_-$  is finite in the limit  $m_i \rightarrow \infty$ ,  $\delta \rightarrow 0$  and  $m_i\delta = \alpha$  fixed. We have

$$\sigma_- = \frac{\alpha m}{2\pi} \int_{-\infty}^0 \frac{(1 - e^{-2\kappa W}) dk}{\kappa - k + \alpha m + (\kappa + k - \alpha m)e^{-2\kappa W}}. \quad (4.36)$$

Making a change of variable  $k \rightarrow -k$  in the integral we find that the surface charge density  $\sigma_-$  is equal to the one computed in Sec. IV A using the screening sum rule (4.17),  $\sigma_- = \sigma$ , as it should be. The screening sum rule (4.17) is then verified.

### 3. The correlations

For both points  $\mathbf{r}_1$  and  $\mathbf{r}_2$  on the boundary (region 1) we compute the charge density correlation function by using

$$\rho_{--}^{(2)T}(\mathbf{r}_1, \mathbf{r}_2) = -m_0^2 |g_{--}(\mathbf{r}_1, \mathbf{r}_2)|^2. \quad (4.37)$$

The Green function  $g_{--}$  given by the Fourier transform of Eq. (4.33) is proportional to  $m_0 = \sqrt{mm_i}$ . Then, the charge density correlation function is proportional to  $m_i^2$ . This gives a well defined surface charge density-surface charge density correlation function

$$\langle \sigma_-(y_1) \sigma_-(y_2) \rangle^T = \delta^2 \rho_{--}^{(2)T}(\mathbf{r}_1, \mathbf{r}_2), \quad (4.38)$$

in the limit  $m_i \rightarrow \infty$ ,  $\delta \rightarrow 0$  and  $m_i\delta = \alpha$  fixed. The final expression for the correlation function is

$$\begin{aligned} \langle \sigma_-(y_1) \sigma_-(y_2) \rangle^T &= - \left[ \frac{m\alpha}{2\pi} \right]^2 \times \\ &\times \left| \int_0^\infty \frac{(1 - e^{-2\kappa W}) e^{iky} dk}{\kappa + k + \alpha m + (\kappa - k - m\alpha) e^{-2\kappa W}} \right|^2, \end{aligned} \quad (4.39)$$

with  $y = y_1 - y_2$ . As before it is interesting to study the decay of the correlations along the  $y$ -axis. The discontinuity of the Fourier transform of the Green function at  $k = 0$  will be translated into a  $1/y$  decay. Then the surface charge correlation will have the asymptotic behavior

$$\langle \sigma_-(y_1) \sigma_-(y_2) \rangle^T \simeq - \frac{\alpha^2}{4\pi^2} \frac{(1 - e^{-2mW})^2}{(1 + \alpha + (1 - \alpha)e^{-2mW})^2} \frac{1}{y^2}, \quad (4.40)$$

and for very large films  $W \rightarrow \infty$

$$\langle \sigma_-(y_1) \sigma_-(y_2) \rangle^T \simeq - \frac{\alpha^2}{4\pi^2(\alpha + 1)^2} \frac{1}{y^2}. \quad (4.41)$$

In relation to the results of Sec. IV A on the asymptotic behavior of the total charge correlation function  $S(\mathbf{r}_1, \mathbf{r}_2)$  inside the film we notice that for  $y \rightarrow \infty$  and in the limit  $W \rightarrow \infty$  the following sum rule is verified

$$\langle \sigma_-(y_1) \sigma_-(y_2) \rangle^T = \alpha^2 \int_0^\infty dx_2 \int_0^\infty dx_1 S(\mathbf{r}_1, \mathbf{r}_2). \quad (4.42)$$

When  $\mathbf{r}_1$  is in region 2 (inside the film) and  $\mathbf{r}_2$  remains on the boundary, the correlation function  $\rho_{--}^{(2)T}$  is given by

$$\rho_{--}^{(2)T}(\mathbf{r}_1, \mathbf{r}_2) = -m_0 m |g_{--}(\mathbf{r}_1, \mathbf{r}_2)|^2, \quad (4.43)$$

with the Green function  $g_{--}$  given by the inverse Fourier transform of Eq. (4.34a). The correlation function  $\rho_{+-}^{(2)T}$  is given by

$$\rho_{+-}^{(2)T}(\mathbf{r}_1, \mathbf{r}_2) = m_0 m |g_{+-}(\mathbf{r}_1, \mathbf{r}_2)|^2, \quad (4.44)$$

with  $g_{+-}$  given by the inverse Fourier transform of Eq. (4.34b). We notice that both correlation functions are proportional to  $m_0^2 = m_i m$ . Then the charge density-surface charge density correlation  $\langle \rho_s(\mathbf{r}_1) \sigma_-(y_2) \rangle^T = \delta \rho_{s-}^{(2)T}(\mathbf{r}_1, \mathbf{r}_2)$  will have a well defined finite limit when  $m_i \rightarrow \infty$ ,  $\delta \rightarrow 0$  and  $m_i\delta = \alpha$ .

We find

$$\begin{aligned} \langle \rho_-(\mathbf{r}_1) \sigma_-(y_2) \rangle^T &= - \frac{\alpha m^3}{\pi^2} \times \\ &\times \left| \int_0^\infty \frac{e^{-\kappa W} \sinh[\kappa(L - x_1)] e^{iky} dk}{\kappa + k + \alpha m + (\kappa - k - \alpha m) e^{-2\kappa W}} \right|^2, \end{aligned} \quad (4.45)$$

and

$$\begin{aligned} \langle \rho_+(\mathbf{r}_1) \sigma_-(y_2) \rangle^T &= \frac{\alpha m}{4\pi^2} \times \\ &\times \left| \int_0^\infty \frac{e^{-\kappa(L+x_1)} [\kappa + k + (\kappa - k) e^{-2\kappa(L-x_1)}]}{\kappa + k + \alpha m + (\kappa - k - \alpha m) e^{-2\kappa W}} dk \right|^2. \end{aligned} \quad (4.46)$$

It is interesting to notice a relation between  $\langle \rho_-(\mathbf{r}_1) \sigma_-(y_2) \rangle^T$  and the surface charge density correlation when both points are at the border, which we might call “continuity”. This relation is

$$\langle \rho_-(x_1 = -L, y_1) \sigma_-(y_2) \rangle^T = \frac{m}{\alpha} \langle \sigma_-(y_1) \sigma_-(y_2) \rangle^T. \quad (4.47)$$

It is also important to study the decay of the correlations along the boundary, when  $|y| = |y_1 - y_2| \rightarrow \infty$ . Here again the discontinuity of the Fourier transform of the Green functions at  $k = 0$  is responsible for a  $1/y^2$  decay of the correlations. The asymptotic behavior of the correlations for  $|y_1 - y_2| \rightarrow \infty$  is

$$\langle \rho_-(\mathbf{r}_1) \sigma_-(y_2) \rangle^T \simeq - \frac{\alpha m [\sinh m(L - x_1)]^2}{[1 + \alpha + (1 - \alpha)e^{-2mW}]^2} \frac{e^{-2mW}}{\pi^2 y^2}, \quad (4.48)$$

and

$$\langle \rho_+(\mathbf{r}_1) \sigma_-(y_2) \rangle^T \simeq \frac{\alpha m [\cosh m(L - x_1)]^2}{[1 + \alpha + (1 - \alpha)e^{-2mW}]^2} \frac{e^{-2mW}}{\pi^2 y^2}. \quad (4.49)$$

For very large films  $W \rightarrow \infty$ , taking now the origin at the boundary  $x_1 \rightarrow x_1 + L$ , the total structure function  $\langle \rho \sigma \rangle^T = \langle \rho_- \sigma_- \rangle^T - \langle \rho_+ \sigma_- \rangle^T$  has the asymptotic behavior

$$\langle \rho(\mathbf{r}_1) \sigma(y_2) \rangle^T \simeq -\frac{\alpha m e^{-2mx_1}}{2\pi^2(\alpha + 1)^2 y^2}. \quad (4.50)$$

We notice that this asymptotic correlation function obeys a sum rule with the charge correlation function  $S(\mathbf{r}_1, \mathbf{r}_2)$  for both points inside the fluid

$$\int_0^\infty S(\mathbf{r}_1, \mathbf{r}_2) dx_2 = \alpha \langle \rho(\mathbf{r}_1) \sigma(y_2) \rangle^T, \quad (4.51)$$

and also a sum rule with the surface charge density correlation when both points are on the boundary

$$\int_0^\infty \langle \rho(\mathbf{r}_1) \sigma(y_2) \rangle^T dx_1 = \alpha \langle \sigma(y_1) \sigma(y_2) \rangle^T. \quad (4.52)$$

The remaining case to complete this study is when the two points are on opposite boundaries, for instance  $\mathbf{r}_2$  in region 1 and  $\mathbf{r}_1$  in region 3. In this case we found that all Green functions are of order  $O(m_0^{-1})$ . Then, the correlation functions given by

$$\rho_{ss'}^{(2)T}(\mathbf{r}_1, \mathbf{r}_2) = m_0^2 g_{ss'}(\mathbf{r}_1, \mathbf{r}_2) g_{s's}(\mathbf{r}_2, \mathbf{r}_1) \quad (4.53)$$

will be finite of order  $O(1)$ . But since there exists a surface charge density at the boundaries, the interesting quantity here is the surface charge correlation function  $\langle \sigma_s \sigma_{s'} \rangle^T = \delta^2 \rho_{ss'}^{(2)T}$  which will vanish in the limit  $\delta \rightarrow 0$ . We have the interesting result: the surface charge densities at opposite boundaries are completely uncorrelated.

To conclude this section let us return to the sum rule (4.24) for the correlations functions along the boundary for  $W \rightarrow \infty$ . If one takes into account all contributions (both particles in the fluid, one particle in the boundary and one in the fluid and both particles in the boundary) to the charge density correlation function, this function should read

$$S_{\text{total}}(\mathbf{r}_1, \mathbf{r}_2) = S(\mathbf{r}_1, \mathbf{r}_2) \quad (4.54a)$$

$$+ \delta(x_1) \langle \sigma(x_1) \rho(\mathbf{r}_2) \rangle^T \quad (4.54b)$$

$$+ \delta(x_2) \langle \sigma(x_2) \rho(\mathbf{r}_1) \rangle^T \quad (4.54c)$$

$$+ \delta(x_1) \delta(x_2) \langle \sigma(x_1) \sigma(x_2) \rangle^T \quad (4.54d)$$

where the structure function  $S(\mathbf{r}_1, \mathbf{r}_2)$  in Eq. (4.54a) contains only the contributions for particles in the fluid, the correlations  $\langle \rho \sigma \rangle^T$  in Eqs. (4.54b) and (4.54c) contain the contribution when one point is on the boundary and the other in the film, and finally the correlation  $\langle \sigma \sigma \rangle^T$

contains the contribution when both particles are on the boundary. The origin is taken on the boundary. Using the asymptotic expressions for the different correlations given by Eqs. (4.25), (4.50) and (4.41) one can check that the sum rule (4.24) is verified:

$$\begin{aligned} \int_0^\infty dx_1 \int_0^\infty dx_2 S_{\text{total}}(\mathbf{r}_1, \mathbf{r}_2) &= -\frac{1}{4\pi^2 y^2} \frac{1 + 2\alpha + \alpha^2}{(\alpha + 1)^2} \\ &= -\frac{1}{4\pi^2 y^2}. \end{aligned} \quad (4.55)$$

For finite  $W$  there exists also a sum rule similar to Eq. (4.24) for *conducting* Coulomb systems [15, 16]. This sum rule reads

$$\int_{-L}^L dx_2 \int_{-L}^L dx_1 S_{\text{total}}(\mathbf{r}_1, \mathbf{r}_2) = -\frac{1}{\beta \pi^2 y^2}, \quad (4.56)$$

for  $|y| \rightarrow \infty$ . From Eqs. (4.9) and (4.10) one can compute the asymptotic behavior of the correlations for both points in the fluid. We find

$$S(\mathbf{r}_1, \mathbf{r}_2) \simeq -\frac{m^2}{2\pi^2 y^2} \frac{\cosh[2m(x_1 + x_2)]}{[\cosh(mW) + \alpha \sinh(mW)]^2} \quad (4.57)$$

Taking into account all contributions from Eqs. (4.40), (4.48) and (4.49) to the total charge correlation function one finds

$$\begin{aligned} \int_{-L}^L \int_{-L}^L S_{\text{total}}(\mathbf{r}_1, \mathbf{r}_2) dx_1 dx_2 &= -\frac{1}{2\pi^2 y^2} \times \\ &\times \frac{\sinh^2 mW + 2\alpha \cosh mW \sinh mW + \alpha^2 \sinh mW}{[\cosh mW + \alpha \sinh mW]^2} \\ &= -\frac{1}{2\pi^2 y^2} \left[ 1 - \frac{1}{[\cosh mW + \alpha \sinh mW]^2} \right]. \end{aligned} \quad (4.58)$$

The sum rule (4.56) is not verified. The discrepancy however is exponentially small when  $W \rightarrow \infty$ . This situation also occurs in the case  $\alpha = 0$  which was studied in Ref. [11]. The two-component plasma is no longer in its conducting phase at  $\Gamma = 2$  when confined in a slab. This is a special property of the two-component plasma at it is not related to the short-range attractive potential near the boundaries. For this reason the sum rule (4.56) is no longer valid. Actually for a Coulomb system in a dielectric phase, the rhs. of the sum rule (4.56) should read  $(-1/\beta \pi^2 y^2)(1 - \epsilon^{-1})$  with  $\epsilon$  the effective static dielectric constant of the system. Then, in our case the system has a effective dielectric constant given by

$$\epsilon = (\cosh mW + \alpha \sinh mW)^2 \quad (4.59)$$

This phenomenon is particular to the two-dimensional two-component plasma and probably should not apply to real three-dimensional soap films.

## V. CONCLUSION

We have studied a toy model for electrolytic soap films. Although this model is very simple and gives only qualitative information for real soap films it is very interesting since it is a solvable model. Our study of the disjoining pressure shows that the charging of the boundaries is responsible of the stability of the film. For strong adhesivity  $\alpha > 1$  the film is stable while for weak adhesivity  $\alpha < 1$  large films are not stable. For  $0 < \alpha < 1$  large films collapse to non-zero width small films. This could be the equivalent of a collapse to a Common Black Films for our two-dimensional model. For  $\alpha = 0$  unstable large films collapse to a film of zero width which could be the equivalent of a Newton Black Film. We can conclude that the Coulomb interaction plays indeed an important role in the stability of large films. This is also the case in the one-dimensional model presented in Ref. [4]. Then it is natural to expect that for real three dimensional films the Coulomb interaction also plays an important role in their stability. Of course in real films there are other important interactions that certainly play a role in the stability of the film and in particular in the stability and structure of black films (both Common Black Films and Newton Black Films) that have not been taken into account in our simplified model.

We also studied the density profiles and correlation functions for this two-dimensional model. The density profile near a boundary shows a classical double layered

structure. A fraction of the anions (soap molecules) are stucked in the boundary creating a first layer of negative surface charge density. The ions in the fluid create the second layer of positive charge and thickness given by the screening length which screens the first layer.

The correlation functions exhibit the usual behavior. In the  $x$ -direction across the film they decay exponentially with the characteristic screening length. In the  $y$ -direction parallel to the boundary they decay algebraically as  $1/y^2$ . The total charge correlation function (taking into account all contributions of particles in the fluid and in the boundary) obeys the usual sum rule for Coulomb fluids near a plane wall when  $W \rightarrow \infty$ . For  $W$  finite, the two-component plasma at  $\Gamma = 2$  is no longer a conductor and therefore fails to satisfy a sum rule for correlations along the boundaries. We also found an interesting new fact: the surface charge densities on opposite boundaries are completely uncorrelated.

## Acknowledgments

G. T. would like to thank B. Jancovici for useful discussions concerning the sum rules of Sec. IV. The authors acknowledge partial financial support from COL-CIENCIAS and BID through project # 1204-05-10078. G. T. acknowledge support from ECOS Nord/ICFES action C00P02 of French and Colombian cooperation.

- 
- [1] O. Belorgey and J. J. Benattar, Phys. Rev. Lett. **66**, 313 (1991).
  - [2] D. Sentenac and J. J. Benattar, Phys. Rev. Lett. **81**, 160 (1998).
  - [3] D. S. Dean and D. Sentenac, Europhys. Lett. **38** 645 (1997)
  - [4] D. S. Dean, R. R. Horgan and D. Sentenac, J. Stat. Phys. **90**, 899 (1998).
  - [5] F. Cornu and B. Jancovici, J. Chem. Phys. **90**, 2444 (1989).
  - [6] B. Jancovici and G. Téllez, J. Stat. Phys. **82**, 609 (1996).
  - [7] P. J. Forrester, J. Stat. Phys. **67**, 433 (1992).
  - [8] G. Téllez, J. Stat. Phys. **104**, 945 (2001).
  - [9] B. Jancovici, G. Manificat and C. Pisani, J. Stat. Phys. **76**, 307 (1994).
  - [10] B. Jancovici and L. Šamaj, J. Stat. Phys. **104**, 755 (2001).
  - [11] B. Jancovici and G. Manificat, J. Stat. Phys. **68**, 1089 (1992).
  - [12] F. Cornu, *Mécanique Statistique Classique de Systèmes Coulombiens Bidimensionnels: Resultats Exacts*, Ph. D. Thesis, Orsay, France (1989).
  - [13] B. Jancovici, J. Stat. Phys. **28**, 43 (1982)
  - [14] B. Jancovici, J. Stat. Phys. **29**, 263 (1982)
  - [15] Ph. A. Martin, Rev. Mod. Phys. **60**, 1075 (1988)
  - [16] P. J. Forrester, B. Jancovici and E. R. Smith, J. Stat. Phys. **31**, 129 (1983).